ISSN 1062-8738, Bulletin of the Russian Academy of Sciences: Physics, 2017, Vol. 81, No. 3, pp. 288–291. © Allerton Press, Inc., 2017.
Original Russian Text © O.B. Perevalova, N.A. Koneva, E.V. Konovalova, E.V. Kozlov, 2017, published in Izvestiya Rossiiskoi Akademii Nauk, Seriya Fizicheskaya, 2017, Vol. 81, No. 3, pp. 315–318.

# Effect of Atomic Ordering on the Role of Grain Boundaries in the Plastic Deformation of $Ni_3Fe$ Alloy

**O.B. Perevalova[a], *, N. A. Koneva[b], E. V. Konovalova[c], and E. V. Kozlov[b]**

[a] *Institute of Strength Physics and Material Science, Siberian Branch, Russian Academy of Sciences, Tomsk, 634021 Russia*

[b] *Tomsk State University of Architecture and Building, Tomsk, 634003 Russia*

[c] *Surgut State University, Surgut, 628499 Russia*

**e-mail: perevalova52@mail.ru*

**Abstract**—The structure of dislocations and the defect structure of grain boundaries and their parameters in $Ni_3Fe$ alloy with short-range order (SRO) and long–range order (LRO) at different stages of plastic deformation are studied by means of transmission diffraction electron microscopy using thin foils and replicas. It is found that atomic ordering reduces the Σ3 twins plasticizing effect, increases the density of grain boundary defects, slows their annihilation during deformation, and intensifies the microstrains at the triple junctions of grain boundaries.

**DOI:** 10.3103/S1062873817030273

## INTRODUCTION

In contrast to monocrystals, the polycrystals of $Ni_3Fe$ alloy with superstructure $L1_2$ display grain boundary brittleness during plastic deformation [1]. In order to solve the problem of grain boundary brittleness in an alloy with superstructure $L1_2$ we must make a comparative study of the development of plastic deformation in its disordered and ordered states.

This work presents the results from studying the structure of dislocations, the defect structure of grain boundaries, and their parameters in $Ni_3Fe$ polycrystal with different states of atomic order at different stages of plastic deformation.

## EXPERIMENTAL

In this work, we used transmission diffraction electron microscopy to study the microstructures of polycrystals. The structure of dislocations and structure of the grain boundaries were investigated using thin foils, while sliding traces were studied using carbon replicas. Parameters of the solid solution (long-range atomic order, parameters of the crystal lattice, and mean-square displacement of atoms) were studied via X-ray diffraction. A description of preparing samples in the state of disorder is presented in Table 1. A description of preparing samples in the state with long-range atomic order (LRO) is presented in Table 2. Deformation was achieved via compression on an Instron unit at a rate of $10^{-2}$ $s^{-1}$ using 3 × 3 × 6 mm samples at room temperature. Deformation curves σ–ε had four stages differing in strain-hardening coefficient: a transition stage and stages II, III and IV [2]. Comparative studies of the development of plastic deformation in alloy polycrystals in the SRO and LRO states were performed at different stages of the σ-ε curve: at strains corresponding to the yield point, the transition stage, and stage II of the deformation curve.

## RESULTS AND DISCUSSION

It is known [4, 7, 8] that in a LRO alloy, the mechanism of deformation is superstructure dislocation, during which antiphase boundaries spread and sitting barriers are likely to form. This results in weak localization of sliding. Dislocation clusters in LRO alloy therefore have no more than three dislocations. The atomic structure of special boundaries in the LRO alloy has features different from those in the SRO alloy. From the viewpoint of our model of a coinciding sites lattice, a grainy antiphase boundary emerges in the plane of coherent special boundaries, raising their energy [9, 10].

### *Yield Point*

In the SRO alloy, dislocation sliding occurs according to sliding systems oriented relative to the boundary plane in such a way that a shearing component emerges in the plane of grain boundaries. The Schmid factor of the main sliding systems, which applies throughout the grain, is not always maximal at this orientation of the grain relative to the axis of deformation. In the LRO alloy, the main sliding systems in the polycrystal grains always have the maxi-

**Table 1.** Alloy heat treatment, stacking fault energy ($\gamma_{sf}$), and average size of grains as the average distance $\langle d \rangle$ between any of the nearest boundaries, regardless of their type

| Alloy | Preprocessing | Annealing to obtain a certain grain size | | | | $\gamma_{sf}$, mJ/m$^2$ | $\langle d \rangle$, μm |
|---|---|---|---|---|---|---|---|
| $Ni_3Fe$ | Homogenizing annealing at $T = 1373$ K for 3 days; forging at $T = 1173$ K for rods; cold rolling with intermediate annealing at $T = 1273$–$1373$ K | Annealing A [3] | | Annealing B [3] | | 40 [4] | 42 |
| | | $T$, K | Duration | $T$, K | Duration | | |
| | | 903 | 3 min | 1023($0.59T_m$) | 3 days | | |
| | | Hardening was conducted after annealing from $T_{an} = 893$ K ($T_{an} > T_K$, where $T_K$ is the temperature of Kurnakov disorder–order transformation $A1 \rightarrow L1_2$, 803 K) [5]. Short–range order (SRO) formed in the alloy after hardening [6]. | | | | | |

**Table 2.** Kurnakov temperature ($T_K$), annealing mode, annealing time, degree of long-range atomic order (η), average size of the anti-phase domains ($\langle D \rangle_{aphd}$), complex stacking fault energy ($\gamma_{csf}$), and crystal lattice parameter ($a$) under conditions of SRO and LRO

| $T_K$, K | Annealing mode | Annealing time | η ± 0.02 | $\langle D \rangle_{aphd}$, nm | $\gamma_{csf}$, mJ/m$^2$ | $a \pm 0.0002$, nm | |
|---|---|---|---|---|---|---|---|
| | | | | | | SRO | LRO |
| 808 [5] | Annealing in the interval of 808–593 at a rate of 5 K per day, followed by cooling in a furnace | Two months | 0.90 | 10 [5] | 105 [7] | 0.3534 | 0.3533 |

mum Schmid factor. Their orientation relative to the grain boundary plane does not meet the condition of shearing in the grain boundary plane. When there are sources of dislocation within the grain boundaries, grain borderline (GBL) defects appear within grain boundaries regardless of the state of the atomic order. In an SRO alloy, the GBL density is commensurate with the density of dislocations in the boundary region. The GBL density within random boundaries is higher than within special boundaries. In the LRO alloy, near-boundary dislocation sliding is localized near the boundary of grains. The GBL density within special boundaries is higher than in random boundaries, though the density of dislocations in the near-boundary region is lower. This is likely due to the specific character of the atomic structure of special boundaries in the LRO alloy, mainly because the grain boundary dislocation is superstructure dislocation.

*Transition Stage ($\varepsilon = 0.04$–$0.05$)*

In the SRO alloy, the Schmid factor of the main sliding systems in the polycrystal grains falls to 0.3. In the LRO alloy, the main sliding systems have Schmid factors in the interval of 0.45–0.5. This shows that the proportion of main sliding systems (which are actually accommodational systems) grows in the SRO alloy, while the accommodation sliding systems in the LRO alloy remain localized near grain boundaries, and the in-grain sliding of dislocations occurs due to in-grain sources. The GBL density in the LRO alloy is twice that in an SRO alloy. The ratio of the density of sliding traces on the surface of a deformed crystal to the GBL density in either state of an alloy is 5–6 (Table 3). That means that the greater GBL density in the LRO alloy is explained by the greater density of sliding traces in the polycrystal grains. The sliding of dislocations in neighboring grains is transferred through the twin Σ3 boundaries of grains in the SRO alloy. It is well known [11] that an increase in the twins shear in the grain boundary sets of disordered solid solutions results in greater plasticity. Studies of sliding traces patterns showed that there is no transfer of sliding through special boundaries in the LRO alloy at the transition stage. In the SRO alloy, extinction contours that reveal torsion curvature χ of the crystal lattice or internal microstrains appear near triple joints. In the LRO alloy, they appear near the facets of special boundar-

**Table 3.** Ratio of the GBL density ($\rho_{gbl}$) and the density of sliding tracks ($n$) in the alloy with SRO and LRO

| Deformation ratio, ε | $\rho_{gbl} \times 10^{-7}$, m$^{-1}$ | | $n \times 10^{-6}$, m$^{-1}$ | | $\rho_{gbl}/n$ | |
|---|---|---|---|---|---|---|
| 0.04–0.05 | SRO | LRO | SRO | LRO | SRO | LRO |
| | 1.5 | 3.3 | 2.4 | 6 | 6 | 5 |

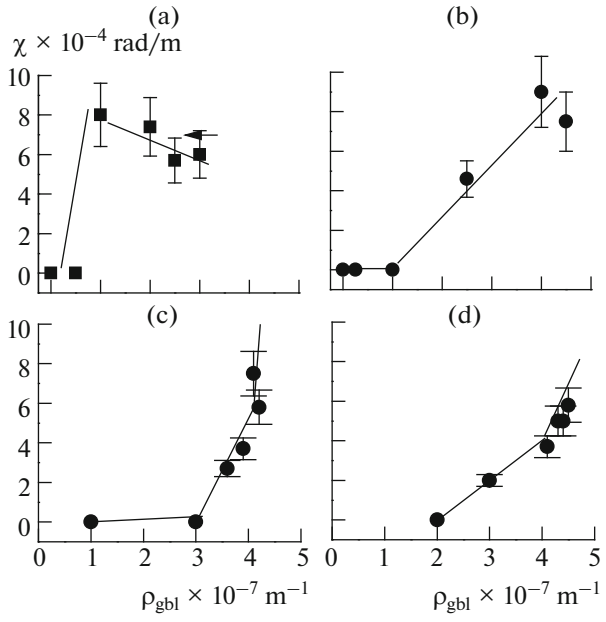


**Fig. 1.** Dependence of $\chi$ on $\rho_{gbl}$ at a distance of 0.1 μm from (a, c) triple junctions of random type grain boundaries and (b, d) facets of special boundaries in $Ni_3Fe$ alloy with (a, b) SRO and (c, d) LRO.

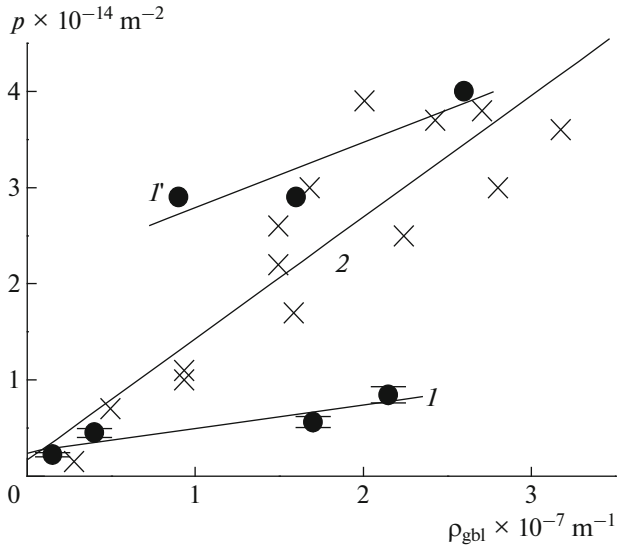


**Fig. 2.** Dependence between $\rho$ and $\rho_{gbl}$ within the boundaries of the (*1*, *1'*) (–●–) random and (*2*) (–×–) special types at (*1*) the yield point and (*1'*) stage II of the deformation curve in the $Ni_3Fe$ alloy with SRO.

ies. The GBL critical density for microstrains in triple joins and on the facets of special boundaries in either state of the alloy is $2–3 \times 10^7$ m$^{-1}$. The structure of dislocations in the grain groups of the SRO alloy is quite heterogeneous. The density of dislocations and the type of the structure of dislocations depend on the size of a grain, the Schmid factor, and the type of grain boundaries. The density of dislocations in individual grains belonging to one group of grains is characterized by a more than 300% difference and stays within the interval of $1.5–5 \times 10^{13}$ m$^{-2}$. In the LRO alloy, the structure of dislocations in a group of grains is more uniform than in the SRO alloy and is classified as tangle or tangle-cell. The density of dislocations in most grains of a group is around $10^{14}$ m$^{-2}$ and does not depend on the size of a grain or the type of grain boundary.

### *Stage II ($\varepsilon \geq 0.1$)*

In both states of the alloy, the increase in GBL density as the degree of deformation grows is accompanied by a rise in torsion curvature $\chi$ of the crystal lattice in triple joints and on the facets of special boundaries (Fig. 1), and by a change of the angle of disorientation of the grain boundaries. The angles of disorientation of the random boundaries increase. The angles of deviation of special boundaries close to $\Sigma 3$ twins are as great as 8°.

However, the accumulation of lattice torsion curvature with the growth of GBL density in triple joints and on the facets of special boundaries differ in the SRO and LRO alloys. In the SRO alloy, a reduction in torsion curvature is observed at triple joints at a distance of 0.1 μm upon a more than $2 \times 10^7$ m$^{-1}$ increase in GBL density (Fig. 1a), while an increase is observed near the facets of special boundaries (Fig. 1b). In the LRO alloy, the rate of torsion curvature accumulation as the GBL density grows is higher in triple joints (Fig. 1c) than on the facets of special boundaries (Fig. 1d). These findings show that there is better agreement between deformation in a grain's body and at grain boundaries in the SRO alloy than in the LRO alloy. Grain boundary sliding toward stage II of deformation curve $\sigma$–$\varepsilon$ lies within the boundary of the random type, resulting in microstrain relaxation in triple joints. In the LRO alloy, grain boundary sliding is observed only on some special boundaries. Grain boundary sliding in the SRO alloy is accompanied by GBL annihilation, as was clear from analyzing the diagram of the dependence of density of dislocations $\rho$ on $\rho_{gbl}$ at the yield point and stage II (Fig. 2). It can be seen from the diagram that there are two parallel dependences $\rho = f(\rho_{gbl})$ for random boundaries at the yield point and at stage II; for the special boundaries, there is only one dependence. This means that within the random boundaries, the annihilation of grain boundary lines occurs simultaneously with the release of dislocations, while the increase in the density of dislocations in the near-boundary region of the special boundaries is due to the action of new grain boundary dislocation sources and thus to the formation of new GBLs.

Active annihilation of the grain boundary lines in situ in an electron microscope was observed by the authors of [12] upon a rise in temperature. The annihilation of GBL upon heating is proportional to the rate of grain boundary diffusion. In the LRO alloy, there is no microstrain relaxation in triple joints or on the facets of special boundaries. The energy of diffusion activation in the LRO alloy is higher than in the SRO alloy [1, 13]. This means that under same conditions, the rate of diffusion is slower (this includes grain boundary diffusion). As a mechanism for reducing the internal strains induced by declinations in triple joints and on the facets of the special boundaries, grain boundary diffusion in the LRO alloy is thus less effective than in the SRO alloy. This is why the increase in the internal strain in the triple joints in the LRO alloy as the degree of deformation grows leads to the formation of grain boundary cracks along the random boundaries.

## CONCLUSIONS

With the atomic ordering of $Ni_3Fe$ alloy, the role of grain boundaries as sources of dislocations changes. In the SRO alloy, grain boundary sources facilitate dislocation sliding by the main sliding systems acting throughout a grain. In the LRO alloy, this only occurs near grain boundaries. The effect the type of boundary has on the development of plastic deformation in a polycrystal also changes. In the LRO alloy, there is no plastifying effect from $\Sigma 3$ twins. The accumulation of defect density within grain boundaries (especially special ones) at the initial stages of the deformation curve, and the weaker annihilation during deformation relative to the SRO alloy, increase the microstrains in triple joints and lead to the formation of grain boundary cracks at random boundaries.

## ACKNOWLEDGMENTS

The work of O.B. Perevalova was supported by the Programs for Basic Scientific Research of the State Academies of Science for 2013–2020; that of E.V. Kozlov, N.A. Koneva, and E.V. Konovalova was partially supported as part of State Task no. 3.295.2014/K of the RF Ministry of Education and Science.

## REFERENCES

1. Popov, L.E. and Kozlov, E.V., *Mekhanicheskie svoistva uporyadochennykh tverdykh rastvorov* (Mechanical Properties of Ordered Solid Solutions), Moscow: Metallurgiya, 1970.
2. Koneva, N.A. and Kozlov, E.V., *Russ. Phys. J.*, 1990, vol. 33, no. 2, p. 165.
3. Arko, A.C. and Liu, Y.H., *Metall. Trans.*, 1971, vol. 2, no. 7, p. 1875.
4. Popov, L.E., Esipenko, V.F., and Koneva, N.A., *Fiz. Met. Metalloved.*, 1975, vol. 40, no. 1, p. 211.
5. Kozlov, E.V., Tailashev, A.S., Shtern, D.M., and Klopotov, A.A., *Sov. Phys. J.*, 1977, vol. 20, no. 5, p. 583.
6. Goman'kov, V.I., Puzei, I.M., and Loshmanov, A.A., *Fiz. Met. Metalloved.*, 1966, vol. 22, no. 1, p. 128.
7. Shoeck, J., *Philos. Mag. Lett.*, 1997, vol. 75, no. 1, p. 7.
8. Popov, L.E., Koneva, N.A., and Tereshko, I.V., *Deformatsionnoe uprochnenie uporyadochennykh splavov* (Strain Hardening of Ordered Alloys), Moscow: Metallurgiya, 1979.
9. Takasugi, T. and Isumi, O., *Acta Metall.*, 1983, vol. 31, no. 8, p. 1187.
10. Perevalova, O.B., Konovalova, E.V., Koneva, N.A., and Kozlov, E.V., *Vliyanie atomnogo uporyadocheniya na zerбnogranichnye ansambli GTsK-tverdykh rastvorov* (Effect of Atomic Ordering on Grain-Boundary Ensembles in FCC Solid Solutions), Tomsk: NTL, 2014.
11. Khodorenko, V.N., Nikitina, N.V., Korotaev, A.D., Karmanchuk, I.V., et al., *Fiz. Met. Metalloved.*, 1990, no. 12, p. 117.
12. Valiev, R.Z., Gertsman, V.Yu., Kaibyshev, O.A., and Sergeev, V.I., *Metallofizika*, 1983, vol. 5, no. 2, p. 94.
13. Larikov, L.N., Geichenko, V.V., and Fal'chenko, V.M., *Diffuzionnye protsessy v uporyadochennykh splavakh* (Diffusion Processes in Ordered Alloys), Kiev: Naukova Dumka, 1975.

*Translated by E. Grishina*